

Oriented Free-Standing Three-Dimensional Silicon Inverted Colloidal Photonic Crystal Microfibers**

By Hernán Míguez, San Ming Yang, Nicolas Tétreault, and Geoffrey A. Ozin*

Electric current control in microelectronics is based on the silicon semiconductor crystal lattice and the existence of an electronic band gap—forbidden energies for the transport of electrons. Silicon can also control the flow of photons when the lattice is constructed at the micrometer scale, giving rise to a complete photonic bandgap (PBG)—a forbidden band of frequencies for the propagation of light.^[1] Because of this phenomenon, silicon promises the same importance in micro-photonics as it has found in microelectronics.^[2] A PBG at optical telecommunication wavelengths has been found in a synthetic 3D silicon photonic lattice having an inverse colloidal crystal structure—a face centered cubic array of air holes in silicon.^[3] Bulk and film morphologies of this material have been formed by a replica process, whereby silicon is deposited within the void spaces of a silica colloidal crystal, followed by silica etching.^[4,5] Herein we describe a self-assembly strategy in which silicon can be fashioned as inverse colloidal photonic crystals in the form of free-standing, oriented rectangular- and V-shaped microfibers. Microspectroscopy of these microfibers is consistent with the existence of a complete PBG near 1.5 μm , making these microfiber constructions interesting as optical components of microphotonic crystal circuits.

The high refractive index glass core with respect to the lower refractive index glass cladding in a conventional optical fiber confines light by total internal reflection. By contrast, glass optical fibers with 1D^[6] and 2D^[7] micrometer scale patterns of microchannels traversing the length of the fiber use a PBG to confine and guide photons, and may find utility for high-capacity transmission of light, switching, and shaping of light pulses or filters for telecommunications. Recent experimental and theoretical developments have shown that oriented colloidal photonic crystals offer opportunities for the fabrication of optical components, such as microlasers,^[8] waveguides,^[9] and superprisms.^[10] Thus if oriented 3D colloidal photonic crystal microfibers could be made, this might enable the realization of these kinds of optical devices. Furthermore any photonic crystal phenomenon in such microfibers would be enhanced, and any device based on them easily integrated into microphotonic technology if the material used was silicon.

A straightforward means of achieving this objective involves the following steps. Silica microspheres with a diameter between ~ 250 nm and ~ 900 nm are first crystallized within the spatial confines of a parallel array of micrometer scale rectangular^[11] microchannels. The microchannels were prepared by patterning a silica or silica-on-silicon flat substrate using the methodology of soft-lithography.^[12] Convection, capillary, and gravitation forces cause the silica microspheres in an ethanolic dispersion to nucleate and grow as well-ordered and oriented face centered cubic (fcc) colloidal crystals exclusively within the microchannels, with the top surface of the colloidal crystal being [111], the sidewalls [11 $\bar{2}$], and the end surfaces [1 $\bar{1}0$].^[11] In order to control the degree of connectivity of the silica spheres in the microchannel, a coating of silica of controlled thickness is deposited by chemical vapor deposition (CVD) and hydrolysis of silicon tetrachloride. Figure 1 shows scanning electron microscopy (SEM) images of a

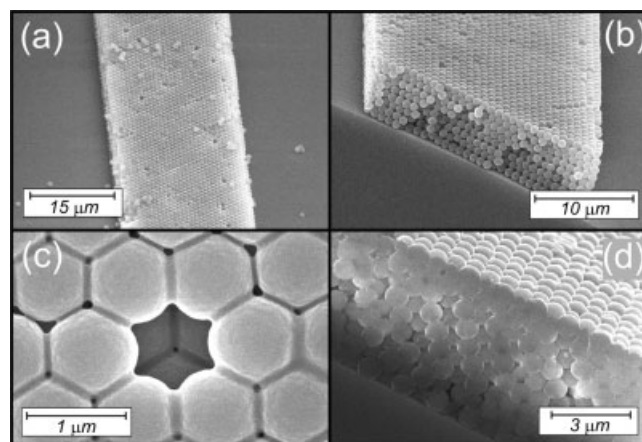


Fig. 1. SEM micrographs of a) rectangular colloidal crystal microchannel. The long-range order of the external surface can be seen; b) detail of a cleaved edge of a colloidal crystal channel with a thickness of eight close packed sphere layers; c) detail of the external [111] surface of the colloidal crystal microchannel after a layer by layer growth of silica is performed by CVD. This treatment enhances the mechanical stability of the silica template and allows control of the degree of interpenetration of the particles; d) detail of a cross section of the microchannel after silica deposition by CVD.

silica colloidal crystal rectangular-shape microchannel template before (Figs. 1a and 1b), and after (Figs. 1c and 1d), the silica infiltration by CVD. Detailed SEM imaging demonstrates in particular the oriented growth of the colloidal crystal, and the high degree of particle necking achieved by the silica CVD treatment can be clearly seen. This provides a high mechanical stability, and allows control of the filling fraction of the template.^[13] Also, it could be used to modify the optical properties of the final silicon inverted colloidal crystal fiber, as explained below.

These silica colloidal crystal microchannels are then infiltrated with silicon in a static chemical vapor deposition reactor using disilane precursor at a pressure of 100 torr and a temperature of 573 K.^[4] The deposited silicon at this temperature forms in the amorphous state and uniformly coats the silica microspheres in a layer-by-layer growth process, which enables excellent control over the volume-filling fraction of

[*] Prof. G. A. Ozin, Dr. H. Míguez, Dr. S. M. Yang, N. Tétreault
Materials Chemistry Research Group, Department of Chemistry
University of Toronto
80 Saint George Street, Toronto, Ontario, M5S 3H6 (Canada)
E-mail: gozin@alchemy.chem.utoronto.ca.

[**] GAO is Government of Canada Research Chair in Materials Chemistry. Financial support for this work from the University of Toronto and the Natural Sciences and Engineering Research Council of Canada is deeply appreciated.

silicon in the tetrahedral and octahedral interstitial spaces of the silica colloidal crystal. These process steps can be performed in a quantitative manner, and prove to be pivotal for precise control of the photonic bandgap properties of the desired oriented 3D silicon inverted colloidal photonic crystal microfibers. To obtain free-standing oriented 3D silicon inverted colloidal photonic crystal microfibers from these parallel microchannel arrays of composite silica–silicon colloidal crystals, all that is required is sacrificial etching of the silica colloidal crystal and the silica on the surface of the substrate using 1% HF/H₂O. This process serves to simultaneously free the silicon inverse colloidal crystal microchannel of the silica that fills its lattice spaces, and removes the silica that holds it onto the substrate, resulting in the formation of a collection of free-standing 3D silicon inverted colloidal photonic crystal microfibers. After washing and drying of the suspension, the microfibers are collected on top of a carbon tape for further electron and optical microscopy analysis.

Representative SEM images of self-supporting rectangular-shaped microfibers are depicted in Figure 2, and clearly show the structurally well-organized inverse silicon colloidal pho-

external surfaces of the fibers (see Fig. 2a, corresponding to a bottom surface of the fiber). Since the silicon growth process takes place layer by layer, the infiltration stops when the external pores of the template are closed (Fig. 2b and c) and before a complete filling of the interstitial space is achieved. The morphology of the bottom surface (Fig. 2b and c), arising from the fact that it is in contact with the substrate, permits observation of the large interconnecting circular windows between spherical cavities, a result of the necking of the starting silica microspheres by silica CVD coating. It should be noted that the thickness of the silica coating grown on top of the spheres will determine both the size of the interconnecting windows and, at the same time, the maximum degree of silicon infiltration achievable. These two parameters strongly affect the optical properties of the resulting silicon inverted colloidal crystal, as shown before,^[3] and must be taken into account when designing the structure for a particular optical function. Figure 3 shows low magnification microscope images of a collection of microfibers presenting different degrees of infiltration. Their length can be several hundreds of micrometers (Fig. 3a). When observed under the optical mi-

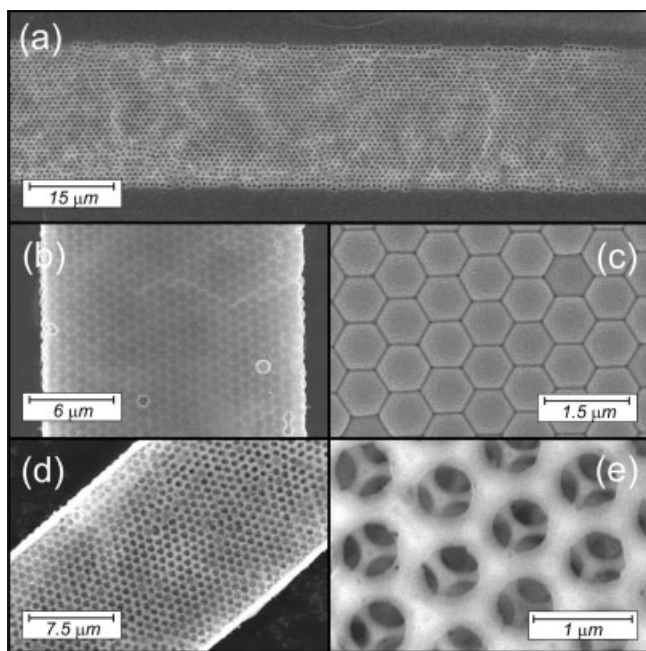


Fig. 2. SEM micrographs of an inverted silicon colloidal crystal fiber: a) Low-magnification image of the bottom surface, observable after the lift off from the substrate. b,c) Details of the top surface of the same kind of fibers, showing that maximum infiltration silicon was achieved (closure of external pores). d,e) Details of the bottom surface of a free-standing silicon inverted colloidal crystal fiber, showing the high degree of connectivity between the spherical cavities resulting from the uniform SiO₂ CVD treatment of the template, which also allows removal of the fibers from the substrate.

tonic lattice. Both the control over the dimensions of the photonic lattice and command of the orientation of the silicon inverted colloidal photonic crystal microfibers result from geometric confinement of silica colloidal crystallization within soft-lithographically pre-defined surface relief microchannel patterns in the substrate. Long-range order is observed in the

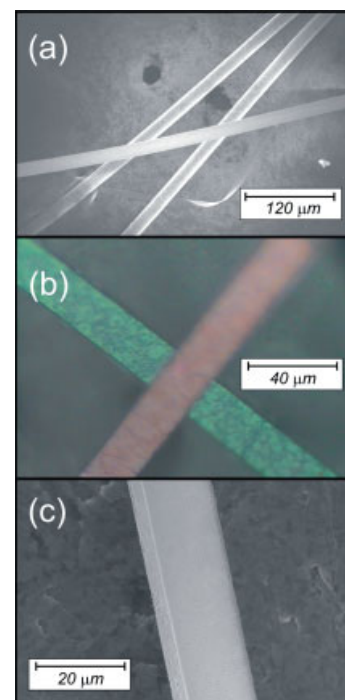


Fig. 3. Micrographs of a collection of different free standing inverted silicon colloidal crystal rectangular-shape fibers: a) Low magnification SEM image of a bunch of fibers collected using a sticky carbon tape. b) Optical picture of two fibers presenting a different degree of infiltration and therefore displaying different colors. c) Closer look by SEM of a slightly tilted fiber, showing explicitly the rectangular shape.

croscopie using a white light source, they display their characteristic reflected colors resulting from the modulation of dielectric constant in the structure. Different degrees of silicon infiltration of the microfiber give rise to different colors (Fig. 3b). The rectangular shape can be clearly seen in the SEM image of a slightly tilted microfiber (Fig. 3c).

The accessibility of the well-defined [111] crystal face of the rectangular-shaped inverted silicon colloidal crystal free-standing microfibers enables micro-optical spectroscopy measurements to be recorded in a near IR Fourier transform instrument, with the incident light source spanning an angle between 15° and 35° with respect to the [111] crystallographic direction of the optical lattice. A typical reflectance spectrum so obtained for the microfibers is shown in Figure 4b, together with the calculated photonic band diagrams (Fig. 4a)

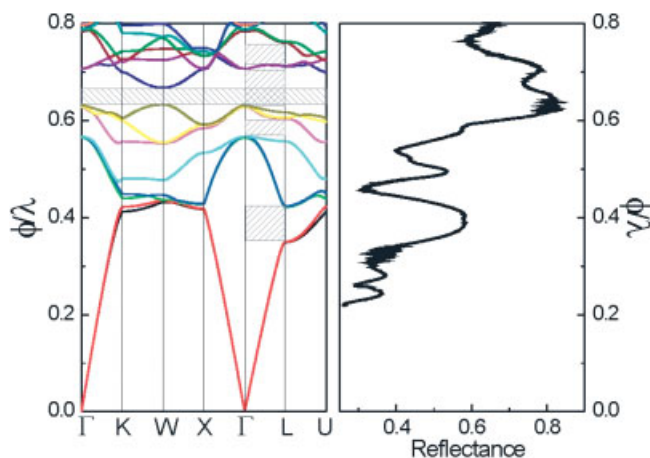


Fig. 4. Left) Photonic band structure of a face centered cubic arrangement of overlapping spherical cavities coated by silicon shells. For the calculation we consider a refractive index of silicon of 3.5 and an inner and outer diameter of the silicon shells of 1.02ϕ and 1.1547ϕ respectively, where ϕ is the spherical cavity center to center distance, which is the same as the diameter of the spheres in the original template. The frequencies are plotted in units of ϕ/λ , λ being the wavelength of light. All the stop bands in the Γ -L direction, which is the one experimentally accessible, are shadowed. The full photonic bandgap is also shown along several principal directions of the first Brillouin zone. Right) Reflectance of a free-standing inverted silicon colloidal crystal fiber obtained from a template made of $\phi = 870$ nm diameter spheres, prior to CVD infiltration of silica. The number and the position of the maxima detected are in good agreement with the calculation. A comparison between theory and experiment indicates that the absolute maximum observed at $\phi/\lambda = 0.635$ in the spectrum ($\lambda \approx 1.4 \mu\text{m}$) should correspond to the full photonic gap. The oscillations observed for frequencies below $\phi/\lambda = 0.3$ are due to the finite size of the silicon photonic crystal fiber along the (111) direction.

along several principal directions in the first Brillouin zone for an fcc lattice of overlapping spherical cavities coated by silicon shells. We consider that maximum infiltration was achieved, as indicated by SEM results. Inspection of the results shows there is good agreement between the observed and computed silicon microfiber stop bands and photonic bandgap, the latter being around $1.4 \mu\text{m}$ and corresponding to the primary maximum in the spectrum. The uniformity of the optical properties measured along the [111] direction and for many different spots along the fibers indicates a high degree of spatial coherence and the low occurrence of defects. However, the effect of the scattering resulting from these defects will be more important when light propagates in the direction parallel to the fiber axis. This will be an important subject of future research, since transmission losses will eventually determine the applicability of these new structures as optical components.

Using a similar procedure, but instead utilizing V-shaped silica colloidal crystal microchannel templates, it is possible to make free-standing oriented inverted silicon colloidal photonic crystal V-shaped microfibers. V-shape surface-relief patterns were prepared by microcontact printing, followed by anisotropic etching of silicon wafers. In this case, colloidal crystallization inside the microchannels was achieved by letting a drop of a suspension of spheres to infiltrate them by capillary forces.^[14] A similar silicon-infiltration and template-etching process to that described for rectangular-shape microchannels was performed. The results are shown in Figure 5. As expected for V-shaped template microchannels with an

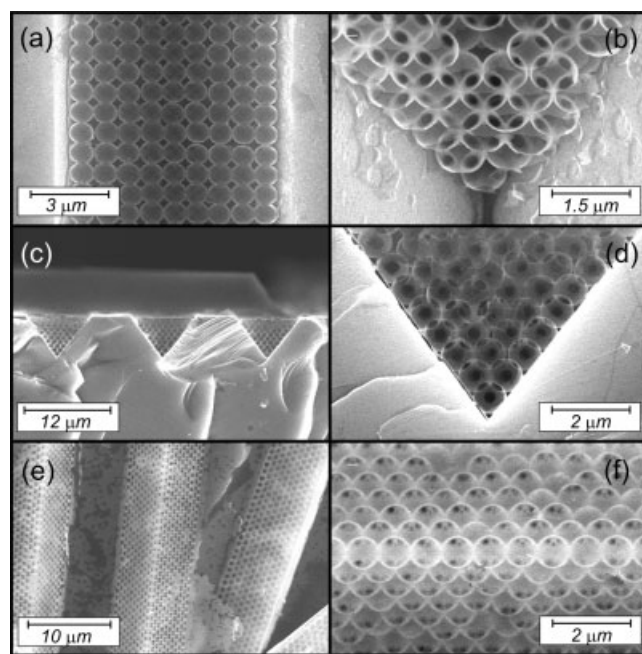


Fig. 5. a) Top view of a triangular Si inverted colloidal crystal fiber confined within a silicon wafer. The 70° angle between the walls of the etched V-shaped groove which hosts the colloidal crystal determines its orientation to be [001] in the direction perpendicular to the wafer, as can be clearly seen in the picture. b) Detail of a cleaved edge of the same fiber as seen from the top, showing explicitly the stacking of (001) planes. c) Low magnification micrograph of a cleaved edge of a silicon wafer containing an array of oriented colloidal crystal fibers. d) Cross section showing the [110] crystallographic direction parallel to the groove. e, f) Free-standing silicon inverted colloidal crystal triangular fiber showing the {111} planes (namely, (-111) and (11-1)), previously in contact with the walls of the groove.

apex angle of 70.6°, the top surface of the V-shaped inverted silicon colloidal photonic crystal microfiber is [001] (Fig. 5a and b), the ends are [110] (Fig. 5c and d) and the sidewalls belong to the {111} family of planes (Fig. 5e and f). Because of the small dimensions of the V-shaped microfiber faces and those of the rectangular-shaped microfiber {112} and {110} faces, there was difficulty in getting micro-optical spectral data for these directions. This challenge will form the subject of a detailed study, in which attempts will be made to map the photonic band structure along these special directions in the Brillouin zone.

Oriented free-standing silicon colloidal photonic crystal microfiber constructs provide a new genre of optical components

with a complete PBG along transverse and longitudinal directions of the microfiber that can be tailored to lie in the optical telecommunication wavelength range. The synthetic strategy outlined herein provides a versatile means for making photonic crystal microfibers with a range of cross-sectional shapes and sizes, microfiber lengths, elemental compositions and photonic lattice dimensions, refractive index contrasts, and optical properties. Just like self-assembled semiconductor nanowires are envisioned as components of future nanocomputers,^[15] one can foresee a myriad of opportunities where photonic crystal microfibers are self-assembled into optical circuits and optically functional devices.

Experimental

Silica microspheres with a diameter between ~250 nm and ~900 nm were synthesized by ammonium hydroxide (Caledon, 28 wt.-%, trace metal grade) catalyzed hydrolytic polycondensation of tetraethoxysilane (Aldrich, 98 %) in ethanolic medium, following the methods described in [16] and [17]. The preparation of the rectangular and V-shaped microchannel surface relief patterns, and the process of colloidal crystallization within them, are described in detail in references [11] and [13], respectively. Both the mechanical stability and the connectivity of the lattice was increased by coating with a continuous layer of SiO₂ the colloidal crystal. This was done using a CVD technique, which involves reaction of bubbled SiCl₄ (Aldrich, 99 %) with the water naturally bonded to the spheres surface. Full details will be presented elsewhere [13]. Amorphous silicon was infiltrated using CVD and later decomposition of disilane (Si₂H₆, 99.99 % Aldrich), using the same experimental set up and following similar recipes to those employed in reference [4], but lowering the gas pressure in the reactor cell down to 100 torr and employing 573 K as decomposition temperature. Lifting the substrate off the silicon microfibers and removal of the silica template was achieved by soaking the silicon infiltrated confined colloidal crystal arrays in an etching 1 wt.-% HF aqueous solution. The entire synthetic route towards the final inverted silicon colloidal crystal microfibers was monitored employing a field emission SEM (Hitachi S-4500).

Received: August 13, 2002
Final version: October 1, 2002

- [1] E. Yablonovitch, *Phys. Rev. Lett.* **1987**, *58*, 2059.
- [2] J. D. Joannopoulos, P. R. Villeneuve, S. Fan, *Nature* **1997**, *386*, 143.
- [3] K. Busch, S. John, *Phys. Rev. E* **1998**, *58*, 3896.
- [4] A. Blanco, E. Chomski, S. Grabtchak, M. Ibisate, S. John, S. W. Leonard, C. López, F. Meseguer, H. Míguez, J. P. Mondia, G. A. Ozin, O. Toader, H. M. van Driel, *Nature* **2000**, *405*, 437.
- [5] Y. A. Vlasov, X. Z. Bo, J. C. Sturm, D. J. Norris, *Nature* **2001**, *414*, 289.
- [6] S. D. Hart, G. R. Maskaly, B. Temelkuran, P. H. Pridaux, J. D. Joannopoulos, Y. Fink, *Science* **2002**, *296*, 510.
- [7] J. C. Knight, J. Broeng, T. A. Birks, P. S. J. Russell, *Science* **1998**, *282*, 1476.
- [8] M. N. Shkunov, Z. V. Vardeny, M. C. DeLong, R. C. Polson, A. A. Zakhdov, R. H. Baughman, *Adv. Funct. Mater.* **2002**, *12*, 21.
- [9] W. M. Lee, S. A. Pruzinsky, P. V. Braun, *Adv. Mater.* **2002**, *14*, 271.
- [10] T. Ochiai, J. Sánchez-Dehesa, *Phys. Rev. B* **2001**, *64*, 245 113.
- [11] a) S. M. Yang, H. Míguez, G. A. Ozin, *Adv. Funct. Mater.* **2002**, *12*, 427.
b) G. A. Ozin, S. M. Yang, *Adv. Funct. Mater.* **2001**, *11*, 95.
- [12] Y. Xia, G. M. Whitesides, *Angew. Chem. Int. Ed.* **1998**, *37*, 551.
- [13] H. Míguez, N. Tetreault, S. M. Yang, B. Hatton, D. Perovic, G. A. Ozin, *Chem Commun.* **2002**, 2737.
- [14] S. M. Yang, G. A. Ozin, *Chem. Commun.* **2000**, 2507.
- [15] Y. Cui, C. M. Lieber, *Science* **2001**, *291*, 851.
- [16] W. Stöber, A. Fink, E. Bohn, *J. Colloid Interface Sci.* **1968**, *26*, 62.
- [17] G. H. Bogush, C. F. Zukoski, *J. Colloid Interface Sci.* **1991**, *142*, 1.

Polymer Gel Light-Modulation Materials Imitating Pigment Cells

By Ryojiro Akashi*, Hiroaki Tsutsui, and Akinori Komura

Stimuli-responsive polymer gels are of great interest to many researchers because these gels demonstrate reversible volume phase transitions^[1,2] in response to external stimuli such as changes in temperature,^[3-5] pH,^[6-8] or light.^[9,10] Recently, many attempts have been reported to use the gels in actuators,^[11-14] artificial muscles,^[15] and other applications.^[16-20] Especially, some applications in light-modulation materials utilizing stimuli-responsive gels are also interesting, e.g., hydrogel opals that consist of microparticle gel networks^[21] and gel particles embedded in crystalline colloidal arrays.^[22] These materials are able to tune the intensity or wavelength of light for transmission or reflection on the basis of Bragg diffraction, and these materials have a potential for application in sensors and optical devices.

Here we present a novel light-modulation material that imitates the behavior of pigment cells and displays a tremendous ability to modulate light absorption. This material is comprised of stimuli-responsive gels to which a high concentration of colorants, such as pigments, is added. The mechanism of the light modulation is due to a reversible volume change of dense colored gel particles, i.e., the light-modulation behavior is caused by a synergetic effect between the change of area of light absorption and the absorption efficiency of colorants in the gels. This material differs from known light-modulation materials in that the color change is induced by the absorption of the colorant itself.

This novel light-modulation material is a simple material system and features various advantages such as excellent light-modulation ability, high durability, and color variety. We anticipate that these novel light-modulation materials may find applications in displays, light modulators, and other optical devices.

Cephalopods such as squids and octopuses have an ability to change their skin color and pattern rapidly. This phenomenon is due to pigment cells present in their skin. The schematic drawing of the structure and behavior of pigment cells in cephalopods is shown in Figure 1. This type of pigment cell consists of an elastic pigment bag, which contains a colorant, and plural muscle fibers. The mechanism for changing the color is based on diffusion and aggregation of colorant that leads to the reversible alteration of the size on the colored bag with the motion of muscles.^[23,24] When the pigment bags expand, the colors appear, and when they contract, the colors bleach out. This type of pigment cell is like a micro-machine in the natural world.

[*] R. Akashi, H. Tsutsui, A. Komura
Intelligent Devices Laboratory, Fuji Xerox Company Limited
1600 Takematsu Minamiashigara, Kanagawa 250-0111 (Japan)
E-mail: ryojiro.akashi@fujixerox.co.jp